

Paired Electrolysis in the Simultaneous Production of Synthetic Intermediates and Substrates

Mark J. Llorente,[†] Bichlien H. Nguyen,[‡] Clifford P. Kubiak,^{*,†} and Kevin D. Moeller^{*,‡}

[†]Department of Chemistry and Biochemistry, University of California, San Diego, 9500 Gilman Drive, Mail Code 0358, La Jolla, California 92093-0358, United States

[‡]Department of Chemistry, Washington University in St. Louis, St. Louis, Missouri 63130, United States

S Supporting Information

ABSTRACT: In electrochemical processes, an oxidation half-reaction is always paired with a reduction half-reaction. Although systems for reactions such as the reduction of CO₂ can be coupled to water oxidation to produce O₂ at the anode, large-scale O₂ production is of limited value. One may replace a low-value half-reaction with a compatible half-reaction that can produce a valuable chemical compound and operate at a lower potential. In doing so, both the anodic and cathodic half-reactions yield desirable products with a decreased energy demand. Here we demonstrate a paired electrolysis in the case of the oxidative condensation of syringaldehyde and *o*-phenylenediamine to give 2-(3,5-dimethoxy-4-hydroxyphenyl)-benzimidazole coupled with the reduction of CO₂ to CO mediated by molecular electrocatalysts. We also present general principles for evaluating current–voltage characteristics and power demands in paired electrolyzers.

In the pursuit of sustainable chemistry, electrolysis reactions are gaining interest because they use electrical energy to drive chemical transformations that maximize atom economy.^{1–3} While such reactions are growing in importance, many of them optimize the efficiency of atom usage without paying similar attention to optimizing the use of energy. Every electrochemical process may be viewed as a complete reaction split into two half-reactions, reduction and oxidation. This fact may be leveraged to allow two desirable half-reactions to be performed simultaneously. In this way, a thoughtful combination of half-reactions may be used to maximize the amount of useful product generated from an electrolysis, thereby maximizing the energy efficiency of the reaction. To date, a number of paired electrochemical reactions of this type have been successfully accomplished.¹ In spite of these successes, however, paired electrochemical reactions remain limited in scope and are greatly underutilized by the larger synthesis community. They are often used for the production of bulk chemicals in processes (e.g., chloralkali) that play little to no role in the production of fine chemicals. Much of this neglect can be attributed to a desire to carefully choose half-reactions on the basis of their complementarity, specific product compatibility, or demand for voltage minimization. In other words, the half-reactions in a paired electrolysis are selected because of the manner in which they fit together. The conclusion is that paired electrochemical reactions are useful for limited specialized

applications; however, this does not need to be the case. In a constant-current (galvanostatic) electrolysis, the working potentials of both the anode and cathode automatically adjust to the potentials of the substrates in solution. Hence, any oxidation or reduction reaction may be paired with any other reduction or oxidation reaction. With this in mind, a paired electrolysis does not need to be developed around specifically matched half reactions but instead can be designed around specific synthetic needs. In principle, an oxidation reaction used in the production of a particular product can be used to also produce a chemical reagent needed elsewhere in the same synthetic sequence or even a different synthesis being conducted within the same company or lab. The result of making the reagent “on-site” in this manner removes the cost of buying, packaging, and shipping these reagents. Rather than looking for specific redox reactions to be paired, we should be using paired electrochemical reactions to improve the sustainability of a wide variety of synthetic transformations. Consider the example illustrated in Figure 1. In this paired electrochemical reaction, two reactions were selected because of a larger effort in our laboratories to valorize biomass. The anodic half-reaction converts syringaldehyde derived from the lignin in raw sawdust into a “privileged” benzimidazole building

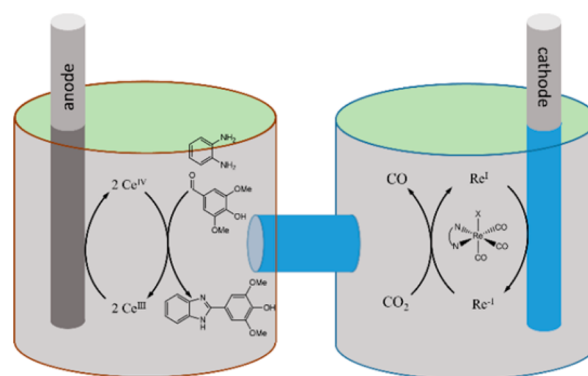


Figure 1. Simplified diagram depicting the half-reactions studied in this paper in a two-compartment cell. Ceric ammonium nitrate acts as the mediating electrocatalyst for the syringaldehyde–diamine condensation reaction, which releases protons into solution. Re(4,4'-ditert-butyl-2,2'-bipyridine)(CO)₃Cl acts as the electrocatalyst for the selective conversion of protons and CO₂ to CO and H₂O.

Received: August 25, 2016

Published: November 8, 2016

block for a variety of applications ranging from pharmaceuticals to vulcanization agents.^{4–6} The cathodic half-reaction generates carbon monoxide from carbon dioxide so as to treat CO₂ as a source for synthetic reagents.^{7–11} The two half-reactions represent parts of a larger effort and were selected because of their independent roles in that effort.^{1,12,13}

Although synthetically driven paired electrolyses of the type illustrated in Figure 1 are easy to design, they are not necessarily ideal from an energetic standpoint. The energy required to run the cell is largely determined by the choice of synthetic transformations to be achieved. Optimization of the energy associated with the paired electrolysis cell is essential for practical applications. This requires reaction conditions for the two half-reactions that optimize the reaction rates with respect to the applied voltage.

Since ample methods for generating renewable electricity exist, the primary goals for a sustainable electrochemical process may be enumerated as (1) sustained electrolysis, (2) high Faradaic yield, (3) optimized power conversion efficiency, (4) current matching of the anodic and cathodic half-reactions, (5) chemical compatibility between the half-reactions, (6) formation of products with higher value than the chemical substrates, and (7) renewably sourced chemical feedstocks. In this Communication, we discuss how these goals can be addressed in the context of the paired electrochemical reaction shown in Figure 1.

To begin such a task, we need to consider electrochemical reactions as whole processes. Take as an example the generic anodic half-reaction A of the form $A_{\text{reduced}} \rightarrow A_{\text{oxidized}}$. This half-reaction is paired with a cathodic half-reaction B of the form $B_{\text{oxidized}} \rightarrow B_{\text{reduced}}$. The total reaction A + B may be described as $(A_{\text{reduced}} + B_{\text{oxidized}}) \rightarrow (A_{\text{oxidized}} + B_{\text{reduced}})$, and the total voltage required to drive this reaction at a given rate may be described as $\Delta V = V_A - V_B$. Optimizing the energy efficiency of the cell requires minimizing ΔV . For most synthetic reactions, this is done by choosing a reaction at the counter electrode that occurs readily at a minimum potential. This lowers the energy demand for the overall process and hence the desired reaction at the working electrode. However, for a paired electrochemical reaction where both reactions are defined by a synthetic goal, this is not an option.

Instead, we focus our aim on minimizing the total voltage applied to maintain the desired reaction rates. In the glass cells used to conduct the paired electrolysis reaction shown in Figure 1, the separator is a fine glass frit wherein small-ion electrolytes such as LiClO₄, LiPF₆, and Et₄NBF₄ give nearly constant series resistances (R_{series}) of $700 \pm 50 \Omega$ across both electrodes regardless of current demand (I) or electrode area. Since the voltage required for electrolysis is typically on the order of 1–3 V, if the current demand is greater than a few milliamperes, IR_{series} becomes the dominant voltage term. Figure 2 shows the steady-state current–voltage behavior for both half-reactions and the total cell as a function of stepped cathodic potentials. The cathode compartment contains 5 mM Re(bipy-tBu)(CO)₃Cl (bipy-tBu = 4,4'-di-*tert*-butyl-2,2'-bipyridine) and saturated carbon dioxide. The anode compartment contains 5 mM ceric ammonium nitrate (CAN), 40 mM syringaldehyde, and 44 mM *o*-phenylenediamine. CAN functions as the electrocatalytic mediator for the oxidative condensation reaction and has a relevant $E_{1/2}$ of 1.0 V vs Ag/AgCl as measured, as demonstrated in Figure S5. An 8:3:1 CH₃CN/THF/MeOH mixed solvent system containing 0.8 M Et₄NBF₄ as the supporting electrolyte was used to ensure solvation of the

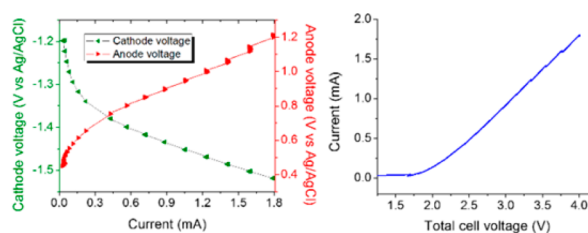


Figure 2. (left) The steady-state current–voltage behavior for each half-reaction was studied by holding the cathode at incrementally decreasing potentials vs an Ag/AgCl reference electrode and measuring the current and anode voltages. The cathode compartment contained 5 mM Re(bipy-tBu)(CO)₃Cl. The anode compartment contained 5 mM CAN, 40 mM syringaldehyde, and 44 mM *o*-phenylenediamine. Data were corrected for solution resistance between the active electrodes and reference electrodes. Under electrolysis conditions, the current rises nearly exponentially as a function of applied voltage at both the anode and the cathode. Higher overpotentials are required at the anode with respect to the cathode, which is indicative of larger barriers and less efficient catalysis. (right) The current–voltage response of the electrolysis cell exhibits exponential behavior at lower current demands and approaches linearity due primarily to separator resistance. The total series resistance between the anode and cathode was measured before and after steady-state measurements to be 740Ω .

substrates and anodic product and to maintain the proton concentration required for the cathodic reaction.^{14,15} With methanol acting as a weak Brønsted acid, the proton concentrations in both compartments are effectively buffered, mitigating adverse chemical potential changes between the compartments during a prolonged bulk electrolysis. For the isolated current–voltage behavior of the half-reactions, the current initially appears exponential as a function of applied potential. This is consistent with kinetically limited electrolytic conditions. For the whole cell, however, the current responds nearly linearly at higher voltages with a slope of $(840 \Omega)^{-1}$, an observation consistent with IR_{series} becoming the dominant term.

Of additional note, as an unintentional but beneficial consequence of using Et₄NBF₄ as the supporting electrolyte and methanol as part of the solvent mixture, the Re catalyst becomes catalytically active at overpotentials less negative than previously reported.¹⁶ While $E_{1/2}$ for the relevant reduction of the catalyst resides at -1.60 V vs NHE, the onset of catalysis occurs at a less negative potential. We attribute this to Et₄N⁺ and methanol facilitating Cl[−] loss from the catalyst and the subsequent stabilization of the active Re[−] species.⁸ Further electrochemical evidence for this can be found in Figures S2–S4.

As evidenced by the current–voltage behavior described above, when driving a paired electrolysis, attempting to arbitrarily increase the rates of product formation by increasing the applied voltage yields limited returns. One must target an acceptable current range that is not so low that the rates of product formation are low and not so high that the energy loss due to resistance becomes prohibitively high or undesirable side reactions predominate. If one were to drive these electrolysis cells with a photovoltaic device, the voltage and current produced by the device would have to be within the range specific to the reaction conditions and equipment used. A custom photovoltaic device was created to produce appropriate voltages and currents by modifying commercially available single-crystalline Solar Made photovoltaic cells. Under direct

solar irradiation, the device performed with a solar energy conversion efficiency of 13% at a maximum power point at 3.1 mA and 4.3 V, as shown in Figure 3.

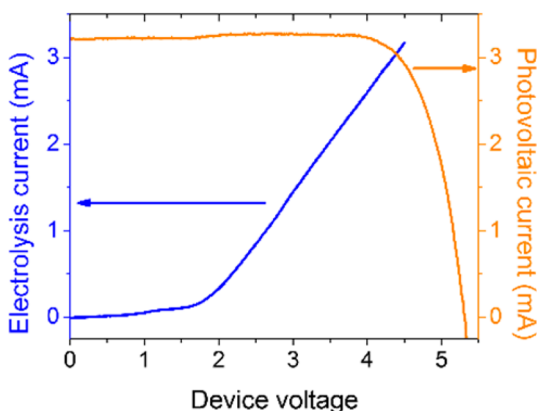


Figure 3. Current–voltage behavior for both the electrochemical cell and the custom photovoltaic device under 98 mW/cm² solar illumination. When the electrolysis cell is driven by the photovoltaic device, the operating current and voltage are determined by where the two curves intersect. The scan rates for both were 20 mV/s.

This device was used to power the electrochemical cell in bulk electrolyses performed under peak mid-day solar flux in La Jolla, CA, under various weather conditions, but in order to mitigate variance between experiments, constant-current electrolyses were performed to simulate the photovoltaic-driven conditions, as shown in Figure S11. A total applied voltage of 4 V was observed for the first half hour with a gradual but progressive increase in demand. In a separate experiment, tracking the current and anode voltages as functions of time for a constant-cathode-voltage electrolysis showed that the increase in voltage demand arose almost entirely from the anode half-reaction, as evidenced in Figure 4.

CO was quantitatively determined by gas chromatography to be evolved with a Faradaic efficiency (FE) of 100% after 2 h of

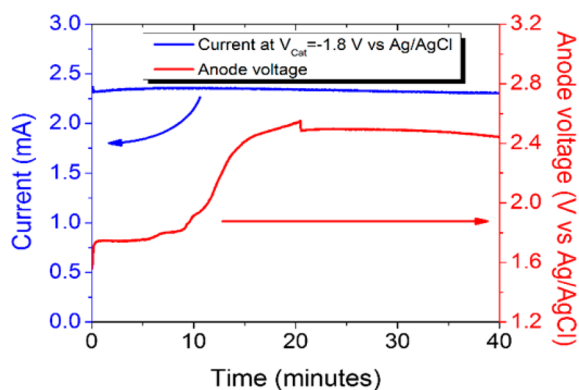


Figure 4. Current and anode voltage (V_a) during constant-cathode-voltage (V_c) electrolysis at low initial substrate concentrations. The cathode compartment contained 5 mM Re(bipy-tBu)(CO)₃Cl. The anode compartment contained 5 mM CAN, 20 mM syringaldehyde, and 22 mM *o*-phenylenediamine. Both compartments were saturated with CO₂. V_c was held at -1.8 V vs Ag/AgCl. The current remained nearly constant throughout electrolysis, consistent with increased voltage demand arising from the anode reaction rather than the cathode reaction. The series resistance between the anode and cathode was measured as 710 Ω before and 720 Ω after the electrolysis.

bulk electrolysis. The syringaldehyde oxidative condensation product was isolated and purified in 65% yield. The structure and purity of the product were confirmed by comparison of NMR and mass spectrometry data with those for the known compound.⁴ Details can be found in the Supporting Information. Two major effects at the anode occur: [1] the condensation product reaches maximum solubility and begins to deposit at the anode, and [2] reactants begin to deplete, increasing the potential required to maintain a constant current.

The pairing of two electrochemical reactions, each of which produces a useful species for chemical synthesis, presents a general paradigm for sustainable production of specialty chemicals in a closed system without the need for sacrificial redox reagents. Such an approach can be used to improve atom economy at the possible expense of energy economy. We show here how appropriate selection of catalysts also improves the energy efficiency of paired electrolysis.

■ ASSOCIATED CONTENT

Supporting Information

The Supporting Information is available free of charge on the ACS Publications website at DOI: 10.1021/jacs.6b08667.

Cyclic voltammograms comparing planar electrodes to glassy carbon rod electrodes with each half-reaction, gas chromatograms for CO quantitation, NMR and high-resolution mass spectra for the anodic product, and voltage vs time and current vs time data for fully sunlight-powered photovoltaic-driven paired electrolysis (PDF)

■ AUTHOR INFORMATION

Corresponding Authors

*ckubiak@ucsd.edu

*moeller@wustl.edu

ORCID

Clifford P. Kubiak: 0000-0003-2186-488X

Notes

The authors declare no competing financial interest.

■ ACKNOWLEDGMENTS

We acknowledge NSF (CHE-1240194/CenSURF) for support of this work and both the UCSD Department of Chemistry and Biochemistry and the Washington University in St. Louis Department of Chemistry for analytical instrumentation.

■ REFERENCES

- (1) Frontana-Urbe, B. A.; Little, R. D.; Ibanez, J. G.; Palma, A.; Vasquez-Medrano, R. *Green Chem.* **2010**, *12*, 2099.
- (2) Yoshida, J.-i.; Kataoka, K.; Horcajada, R.; Nagaki, A. *Chem. Rev.* **2008**, *108*, 2265.
- (3) Sperry, J. B.; Wright, D. L. *Chem. Soc. Rev.* **2006**, *35*, 605.
- (4) For the previous electrochemical reaction, see: Nguyen, B. H.; Perkins, R. J.; Smith, J. A.; Moeller, K. D. *J. Org. Chem.* **2015**, *80*, 11953.
- (5) For the utility of the benzimidazole ring skeleton, see: (a) Cole, D. C.; Gross, J. L.; Comery, T. A.; Aschmies, S.; Hirst, W. D.; Kelley, C.; Kim, J.-I.; Kubek, K.; Ning, X.; Platt, B. J.; Robichaud, A. J.; Solvibile, W. R.; Stock, J. R.; Tawa, G.; Williams, M. J.; Ellingboe, J. W. *Bioorg. Med. Chem. Lett.* **2010**, *20*, 1237. (b) Bressi, J. C.; de Jong, R.; Wu, Y.; Jennings, A. J.; Brown, J. W.; O'Connell, S.; Tari, L. W.; Skene, R. J.; Vu, P.; Navre, M.; Cao, X.; Gangloff, A. R. *Bioorg. Med. Chem. Lett.* **2010**, *20*, 3138. (c) Penning, T. D.; Zhu, G. D.; Gandhi, V. B.; Gong, J.; Liu, X.; Shi, Y.; Klinghofer, B.; Johnson, E. F.; Donawho, C. K.; Frost, D. J.; Bontcheva-Diaz, V.; Bouska, J. J.; Osterling, D. J.

Olson, A. M.; Marsh, K. C.; Luo, Y.; Giranda, V. L. *J. Med. Chem.* **2009**, *52* (2), 514. (d) Yenjerla, M.; Cox, C.; Wilson, L.; Jordan, M. A. *J. J. Pharmacol. Exp. Ther.* **2009**, 328, 390.

(6) For the closely related benzthiazoles (made using the same reaction), see: (a) Carpenter, R. D.; Andrei, M.; Aina, O. H.; Lau, E. Y.; Lightstone, F. C.; Liu, R.; Lam, K. S.; Kurth, M. J. *J. Med. Chem.* **2009**, *52* (1), 14. (b) Ammazalorso, A.; Giancristofaro, A.; D'Angelo, A.; De Filippis, B.; Fantacuzzi, M.; Giampietro, L.; Maccallini, C.; Amoroso, R. *Bioorg. Med. Chem. Lett.* **2011**, *21*, 4869. (c) Vu, C. B.; Milne, J. C.; Carney, D. P.; Song, J.; Choy, W.; Lambert, P. D.; Gagne, D. J.; Hirsch, M.; Cote, A.; Davis, M.; Lainez, E.; Meade, M.; Normington, K.; Jirousek, M. R.; Perni, R. B. *Bioorg. Med. Chem. Lett.* **2009**, *19*, 1416. (d) Bowyer, P. W.; Gunaratne, R. S.; Grainger, M.; Withers-Martinez, C.; Wickramasinghe, S. R.; Tate, E. W.; Leatherbarrow, R. J.; Brown, K. A.; Holder, A. A.; Smith, D. F. *Biochem. J.* **2007**, *408*, 173. (e) Stevens, M. F. G.; McCall, C. J.; Lelieveld, P.; Alexander, P.; Richter, A.; Davies, D. E. *J. Med. Chem.* **1994**, *37* (11), 1689. (f) Bradshaw, T. D.; Westwell, A. D. *Curr. Med. Chem.* **2004**, *11*, 1009. (g) Song, E. Y.; Kaur, N.; Park, K. M.; Jin, Y.; Lee, K.; Kim, G.; Lee, K. Y.; Yang, J. S.; Shin, J. H.; Nam, K. Y.; No, K. T.; Han, G. *Eur. J. Med. Chem.* **2008**, *43*, 1519.

(7) Li, K.; An, X.; Park, K. H.; Khraisheh, M.; Tang, J. *Catal. Today* **2014**, *224*, 3.

(8) Grice, K. A.; Kubiak, C. P. *Adv. Inorg. Chem.* **2014**, *66*, 163.

(9) Kim, D.; Sakimoto, K. K.; Hong, D.; Yang, P. *Angew. Chem., Int. Ed.* **2015**, *54*, 3259.

(10) Kondratenko, E. V.; Mul, G.; Baltrusaitis, J.; Larrazabal, G. O.; Perez-Ramirez, J. *Energy Environ. Sci.* **2013**, *6*, 3112.

(11) Martin, A. J.; Larrazabal, G. O.; Perez-Ramirez, J. *Green Chem.* **2015**, *17*, 5114.

(12) Suga, S.; Okajima, M.; Fujiwara, K.; Yoshida, J.-i. *QSAR Comb. Sci.* **2005**, *24*, 728.

(13) Guenot, B.; Cretin, M.; Lamy, C. *J. Appl. Electrochem.* **2015**, *45*, 973.

(14) Kumar; Smieja, J. M.; Sasayama, A. F.; Kubiak, C. P. *Chem. Commun.* **2012**, *48*, 272.

(15) Keith, J. A.; Grice, K. A.; Kubiak, C. P.; Carter, E. A. *J. Am. Chem. Soc.* **2013**, *135*, 15823.

(16) Smieja, J. M.; Kubiak, C. P. *Inorg. Chem.* **2010**, *49*, 9283.